International Journal of Thermal Sciences 81 (2014) 84–93

Contents lists available at ScienceDirect

International Journal of Thermal Sciences

journal homepage: www.elsevier.com/locate/ijts

Comparison of convective heat transfer coefficient and friction factor of TiO_2 nanofluid flow in a tube with twisted tape inserts

W.H. Azmi [a,1], K.V. Sharma [b,*], P.K. Sarma [c], Rizalman Mamat [a,1], Shahrani Anuar [a,1]

[a] Faculty of Mechanical Engineering, Universiti Malaysia Pahang, 26600 Pekan, Pahang, Malaysia
[b] Department of Mechanical Engineering, University Technology Petronas, Bandar Seri Iskandar, 31750 Tronoh, Perak, Malaysia
[c] GITAM University, Rishikonda, Visakhapatnam 530045, India

ARTICLE INFO

Article history:
Received 1 August 2013
Received in revised form
15 January 2014
Accepted 3 March 2014
Available online 12 April 2014

Keywords:
TiO_2 nanofluid
Heat transfer coefficient
Friction factor
Twisted tape
Advantage ratio

ABSTRACT

Nanofluids have gained extensive attention due to their role in improving the efficiency of thermal systems. The present study reports a further enhancement in heat transfer coefficients in combination with structural modifications of flow systems namely, the addition of tape inserts. Experiments are undertaken to determine heat transfer coefficients and friction factor of TiO_2/water nanofluid up to 3.0% volume concentration at an average temperature of 30 °C. The investigations are undertaken in the Reynolds number range of 8000–30,000 for flow in tubes and with tapes of different twist ratios. A significant enhancement of 23.2% in the heat transfer coefficients is observed at 1.0% concentration for flow in a tube. With the use of twisted tapes, the heat transfer coefficient increased with decrease in twist ratio for water and nanofluid. The heat transfer coefficient and friction factor are respectively 81.1% and 1.5 times greater at $Re = 23{,}558$ with 1.0% concentration and twist ratio of 5, compared to values with flow of water in a tube. An increase in the nanofluid concentration to 3.0% decreased heat transfer coefficients to values lower than water for flow in a tube and with tape inserts. A thermal system with tape insert of twist ratio 15 and 1.0% TiO_2 concentration gives maximum advantage ratio, if pressure drop is considered along with enhancement in heat transfer coefficient.

1. Introduction

Traditionally, heat transfer coefficients have been determined both numerically and experimentally over a wide range of Reynolds and Prandtl numbers involving single phase fluids. The performance of thermal equipment operating with fluids such as water, ethylene glycol and oils, has reached the limit. Various methods for heat transfer enhancement have been developed over the years either to provide high heat flux in a limited space or to optimize the size of the equipment. However, the need for miniaturization of thermal equipments has shifted the focus to the development of new high performance fluids with thermal conductivities higher than those of the conventional liquids. These high performance fluids can contribute to the evolution of space-saving yet cost effective thermal equipments with higher competitiveness in the global market.

Heat transfer enhancements can be achieved through active and passive methods as suggested by Ahuja [1] and Bergles [2]. Active heat transfer enhancement is achieved by the application of external energy on the fluid. Passive enhancement is attained by increasing the fluid surface area, providing artificially roughed surface, introducing swirl flow with twisted tape inserts, convoluted or twisted tube, or by the use of additives in liquids and gases. Of the passive methods, the heat transfer enhancement with nanofluid is highly encouraging. The nanofluids are prepared by dispersing high thermal conducing ultrafine particles of nanometer size in base liquids such as water, thereby enhancing the effective thermal conductivity of the fluid.

Choi and Tran [3] reported studies on heat transfer enhancement undertaken with micron size particles in certain base liquids. The use of these liquids posed problems like clogging, erosion of pipe lines and greater power requirements for pumping compared to base liquid. Further, agglomeration and resettlement of particles posed a severe maintenance problem. In contrast, experiments undertaken with nanofluids showed heat transfer augmentation without any substantial increase in pumping power requirement and associated practical problems.

* Corresponding author.
E-mail addresses: wanazmi2010@gmail.com (W.H. Azmi), kvsharmajntu@gmail.com (K.V. Sharma), sarmapk@yahoo.com (P.K. Sarma), rizalman@ump.edu.my (R. Mamat), shahrani@ump.edu.my (S. Anuar).
[1] Tel.: +60 9424 6338; fax: +60 9424 2202.

http://dx.doi.org/10.1016/j.ijthermalsci.2014.03.002
1290-0729/

Early experiments with Al_2O_3, SiO_2 and TiO_2 nanofluids were undertaken by Masuda et al. [4] to determine the effect of concentration on thermal conductivity. They reported a 30% and 10% increase in thermal conductivity respectively for Al_2O_3 and TiO_2 nanofluids at 4.0% concentration. However, the thermal conductivity enhancement was observed to be significantly lower with SiO_2 nanofluid when compared to other nanofluids.

Pak and Cho [5] determined viscosity and thermal conductivity with 13 nm Al_2O_3 and 27 nm TiO_2 nanoparticles dispersed in water at different concentrations. They observed the influence of particle size and nanofluid concentration on enhancements in viscosity. Turgut et al. [6] determined the viscosity of 21 nm TiO_2 nanoparticles dispersed in deionized water for concentrations up to 3.0% in the temperature range of 13–55 °C. The nanofluid thermal conductivity with 3.0% concentration at 13 °C is 7.4% greater than water. They observed an enhancement in viscosity with TiO_2 nanofluid is greater than the enhancements in thermal conductivity. Subsequent studies involving viscosity and thermal conductivity determination by He et al. [7] decisively indicated that variations in thermal conductivity of TiO_2/water nanofluid have a greater impact on heat transfer coefficient than changes in viscosity.

The parameters influencing nanofluid heat transfer coefficients have been determined experimentally by He et al. [8]. They observed an increase in the convective heat transfer coefficients at varying concentrations of TiO_2 nanofluid under laminar and turbulent flow conditions. They concluded that the influence of concentration on heat transfer coefficient is significant in the turbulent than in the laminar region.

The variation of Nusselt with Reynolds number undertaken with 15 nm TiO_2 nanoparticles in water for concentrations up to 2.0% has been determined by Kayhani et al. [9]. An enhancement of 8.0% in heat transfer coefficient is observed at turbulent Reynolds number of 11,800 with 2.0% nanofluid concentration. Arani and Amani [10] determined turbulent heat transfer coefficients and pressure drop with 30 nm TiO_2/water nanofluid with concentrations in the range of 0.2%–2.0%, and Reynolds numbers between 8000 and 51,000. The experimental results indicated a maximum thermal performance factor of 1.8 at 2.0% concentration at a Reynolds number of 47,000. All these investigators observed heat transfer enhancements with nanofluid concentration.

A decrease in turbulent heat transfer coefficients has been observed by Duangthongsuk and Wongwises [11] with 27 nm TiO_2 particles dispersed in water. They observed heat transfer coefficients to increase with Reynolds number for concentration up to 1.0%. A decrease in heat transfer coefficients was observed at 2.0% concentration, however the values are greater than the base liquid water. The reasons for the decrease in heat transfer coefficient are not stated. The experimental observations of Pak and Cho [5] with 13 nm Al_2O_3 nanofluid also indicate a decrease in heat transfer coefficient at 2.78% concentration. The experiments were undertaken by Refs. [11,5] at 25 °C. Studies by Azmi et al. [12] with SiO_2 nanofluid also indicated a decrease in heat transfer coefficient at an average temperature of 30 °C when the concentration was enhanced to 3.0% with nanoparticles of 22 nm size. Most of the studies undertaken with TiO_2 nanofluid are limited to the determination of properties and heat transfer coefficients for flow in a plain tube.

Modification of flow dynamics with the insertion of twisted tape in a tube for flow of nanofluid in the transition range of Reynolds number was undertaken by Sharma et al. [13]. The tape disrupts the boundary layer formation and induces turbulence even at low flow rates which is a good strategy to achieve high heat transfer rates. Sharma et al. [13] established that 0.1% Al_2O_3 nanofluid flowing in a tube with a tape of twist ratio five, the heat transfer coefficient enhanced by 11.84% at Reynolds number of 3000 and 15.80% at Reynolds number of 9000 compared to flow in the tube without inserts. At the same nanofluid concentration, twist ratio and for Reynolds numbers of 3000 and 9000, the friction factors enhanced by 3.32% and 16.65% respectively compared to flow in a tube. Further investigation for the determination of heat transfer coefficients with a twisted tape insert in the turbulent range of Reynolds number are due to Sundar and Sharma [14]. They observed the enhancement in heat transfer coefficient and friction factor to be respectively 11.16% and 1.09 times compared to flow in a tube with 0.5% Al_2O_3 nanofluid at $Re = 17{,}000$ and twist ratio of 5.0.

Wongcharee and Eiamsa-ard [15] estimated heat transfer enhancement for CuO nanofluid flow in a corrugated tube with twisted tape insert. They reported an increase in convective heat transfer coefficient and friction factor undertaken in the Reynolds number range of 6200–24,000 and concentration in the range of 0.3–0.7%. At 0.5% nanofluid concentration, for $H/D = 5.3$ and $Re = 17{,}000$, the heat transfer coefficient increased by 46.0%, whereas the friction factor is 3.46 times higher compared to flow in a tube. Studies involving altered flow dynamics for heat transfer enhancement with twisted tape inserts have not been reported with TiO_2 nanofluid.

Experimental studies [13–15] were undertaken with Al_2O_3 and CuO nanofluids for a maximum concentration of 0.7% with twisted tape inserts. Studies involving TiO_2 nanofluid for a wide range of concentrations and twist ratios have not been reported till now. Hence experiments are undertaken with TiO_2 nanofluid for volume concentrations up to 3.0% in the turbulent range of Reynolds number. It is intended to determine the effect of concentration on the maximum heat transfer coefficient for flow in a tube and with twisted tape insert. The experimental parameters that foster enhanced thermal performance considering pressure drop of nanofluid for flow in a tube and with twisted tape insert is intended to be determined.

2. Preparation of nanofluid

TiO_2 water based nanofluid contains anatase TiO_2 nanoparticles with 99% purity procured from US Research Nanomaterials, Inc. is used in the experiments after appropriate dilution. It was supplied with an initial concentration of 40% by weight at a pH of 5.5. The nanofluid supplied in weight concentration ω is converted to volume concentration ϕ with Eq. (1). In the calculations, the thermal conductivity, density and specific heat of TiO_2 nanoparticle are taken as 8.4 W/m K, 4175 kg/m^3 and 692 J/kg K respectively as given by Pak and Cho [5]. About 15 L of the nanofluid is prepared to the desired concentration by dilution for the conduct of heat transfer experiments. The volume of distilled water ΔV to be added for attaining a desired concentration ϕ_2 is evaluated with Eq. (2) with the values of V_1 and ϕ_1 known a priory. For example, 3.3 L of TiO_2 is diluted with 11.7 L of water to attain 15 L of nanofluid for obtaining 3.0% volume concentration.

$$\phi = \frac{\omega\rho_w}{(1-\frac{\omega}{100})\rho_p + \frac{\omega}{100}\rho_w} \tag{1}$$

$$\Delta V = (V_2 - V_1) = V_1\left(\frac{\phi_1}{\phi_2} - 1\right) \tag{2}$$

Nanofluid in the concentration range of 0.5–3.0% is prepared in this manner. They are subjected to mechanical and ultrasonic homogenization with NSB-Scientz-IID of 950 W maximum rating for 2 h at all concentrations and observed for dispersion stability. The samples prepared in this manner are observed to be stable for more than a week.

The thermo physical properties of nanofluids such as thermal conductivity and viscosity at each concentration are determined respectively with KD2 Pro thermal property analyzer and

Table 1
The measured value of properties at 30 °C.

Concentration, ϕ	Thermal conductivity ratio, K_r	Absolute viscosity ratio, μ_r
0.5	1.041	1.128
1	1.048	1.195
1.5	1.056	1.240
2	1.066	1.274
2.5	1.067	1.364
3	1.072	1.394

Brookfield LVDV-III Ultra Rheometer. The measured data of thermal conductivity and viscosity ratios are presented in Table 1. The description of KD2 Pro and Brookfield Rheometer are respectively presented by Mintsa et al. [16] and Namburu et al. [17]. The KD2 Pro uses transient line heat source to measure the thermal properties of solids and liquids. It consists of a handheld controller (microcontroller and power control) and two different sensors each for measuring the thermal conductivity of solids and liquids. The apparatus meets the standards of both ASTM D5334 and IEEE 442-1981. A Memmert water bath is used to maintain a constant temperature within 0.1 °C. The sensors are calibrated by determining the thermal conductivity of distilled water and glycerin. In order to ensure that measurement error lies within 5%, a minimum of five measurements are taken at each concentration and temperature as explained by Ding et al. [18] and He et al. [8]. The measured values at 27 °C are 0.610 and 0.280 W/mK respectively, for distilled water and glycerin, which are in agreement with values of 0.613 and 0.285 W/mK, respectively as given by Cengel et al. [19], within ±5% accuracy. The sensor of the viscometer is calibrated with distilled water. The measured value of viscosity for distilled water is 0.85 at 25 °C agrees well with the standard value of 0.9 with ±6% accuracy. Based on the agreement for water, nanofluid properties are evaluated at different concentrations and temperatures. The density and specific heat of nanofluid are estimated based on mixture relations given by

$$\rho_{nf} = \phi\rho_p + (1-\phi)\rho_w \tag{3}$$

$$C_{nf} = \frac{(1-\phi)(\rho C)_w + \phi(\rho C)_p}{(1-\phi)\rho_w + \phi\rho_p} \tag{4}$$

3. Experimental apparatus

The schematic diagram of the experimental setup and the twisted tape is shown in Fig. 1. The setup consists of a chiller, collecting tank, water pump, flow meter, pressure transducer, control panel, and test section. A copper tube of 1.5 m length having ID = 16 mm and OD = 19 mm enclosed with heaters and ceramic fiber insulation constitute the test section. The twisted tapes are manufactured with aluminum strips of 1 mm thick and 16 mm wide as shown in Fig. 1(b). It was fabricated for different twist ratio of 5, 10 and 15 with the width, H of 0.08 m, 0.16 m and 0.24 m respectively. The heat conduction in the aluminum tape along its length is assumed to be negligible.

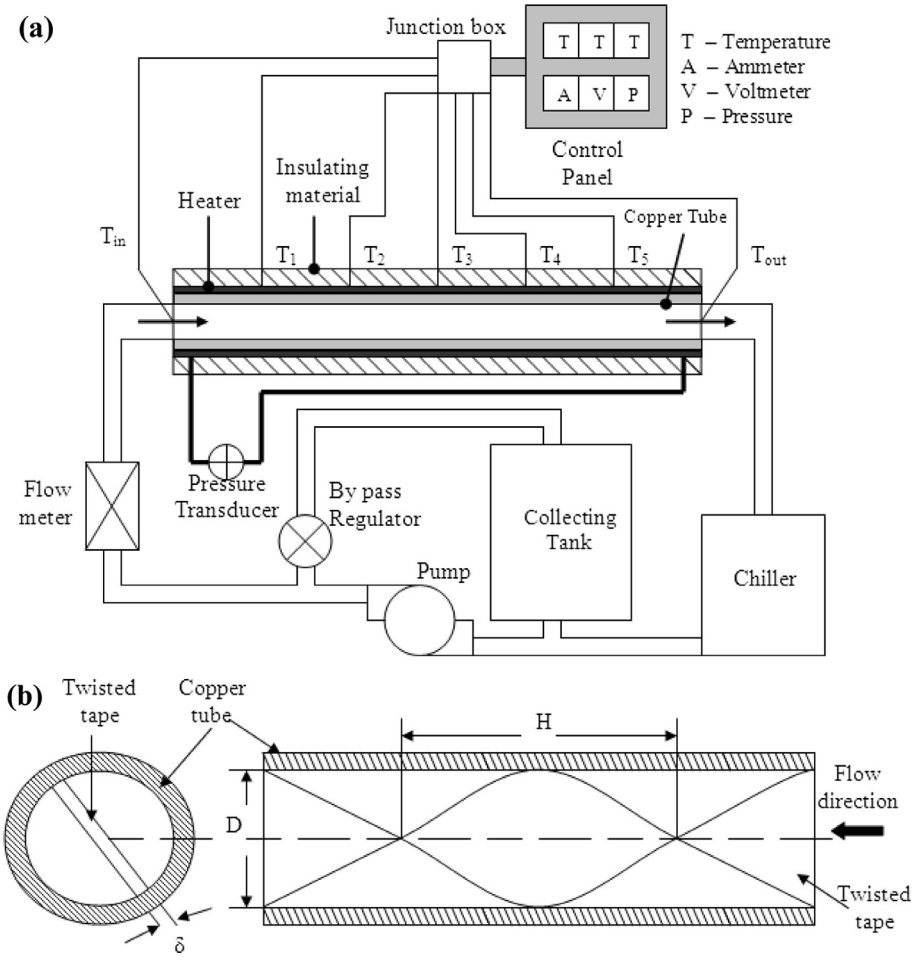

Fig. 1. (a) Schematic diagram of the experimental setup. (b) Configuration of twisted tape.

The working liquid is circulated with a pump of 0.5 horse power rating to force the fluid through the copper tube. The liquid is stored in a collecting tank made of stainless steel of 30 L capacity. Uniform heating of the 1.5 m copper tube is achieved by wrapping it with two nichrome heaters each of 1.5 kW maximum electric rating. The tube is enclosed in ceramic fiber insulation to minimize heat loss to the atmosphere. K-type thermocouples are attached to the test section at the inlet, outlet and on the surface at 0.25, 0.5, 0.75, 1.0 and 1.25 m from the inlet of the tube to record temperatures at various locations. A flow meter capable of measuring in the range of 5–16 LPM is connected to the test section. A chiller of 1.4 kW maximum capacity is connected to the collecting tank to regulate the inlet temperature of the liquid to a set/desired value. A pressure transducer connected across the test section records the pressure drop. The total length of the fluid flow considering the flexible piping is approximately 4.0 m which ensures fully turbulent flow condition at the entry to the test section.

A constant value of 600 W is supplied by the heaters to the test section. The chiller is adjusted to attain a liquid average temperature of 30 °C in the test section with a maximum variation of ±1 °C. The outer surface temperature of the insulated test section is monitored and observed to vary between 27 and 29 °C. The heat loss from the test section is estimated to be less than 1% of heat input. Hence the heat loss to the atmosphere is neglected. A data logger is connected to record the surface temperature of the copper tube (test section) and the inlet and outlet temperatures of liquid every five second to determine the state of the experiment. At steady state, the temperatures, the flow rate and the power input to the heater are recorded. The uncertainties in the measuring instruments are given as Appendix 1.

Experiments are undertaken at different flow rates to determine the pressure drop and heat transfer coefficients of nanofluid for a maximum concentration of 3.0%. The friction factor and heat transfer coefficients are estimated using Darcy pressure drop and Newton's law of cooling relations. Heat transfer coefficients and friction factor are determined for water and TiO_2/water nanofluid at various mass flow rates in tube and with twisted tape insert. The maximum and minimum error in the experimental data is presented as Appendix 2.

4. Results and discussion

4.1. Nanofluid stability

The measurement of pH, electrical conductivity and images from Transmission Electron Microscopy (TEM) were undertaken in order to determine the condition of nanofluid agglomeration, dispersion and stability. The stability of nanofluid is strongly influenced by the pH value. Murshed et al. [20] stated that the solution chemistry of TiO_2/water based nanofluid is neutral in nature. The initial pH value of procured TiO_2/water nanofluid is 5.5. However, the pH varied between 6.9 and 7.7 in the range of 0.5–3.0% volume concentration prepared on dilution. The size, shape and stability of the nanoparticles can be observed from the TEM photographs presented as Fig. 2a–f taken before and after the conduct of experiment for three different concentrations. The supplier specified the particle size to vary between 30 and 50 nm. The surface area of the nanoparticles from TEM images is used to determine the average size of the particle. The cross sectional area of nanoparticle was also determined using Image Processing and Analysis in Java (Image J) software. The average size of TiO_2 nanoparticle suspension in water is determined to be 50 nm. The shape of the particles is non-spherical and the particles are dispersed without agglomeration. To further establish the stability, the electrical conductivity of a sample nanofluid is determined. Sarojini et al. [21] stated that the stability of nanofluid depends critically on the surface charge of nanoparticles which is related to electrical conductivity. The values of electrical conductivity is measured before and after the conduct of experiment. A good agreement of the values can be observed from Fig. 3 confirming the stability of the nanofluid.

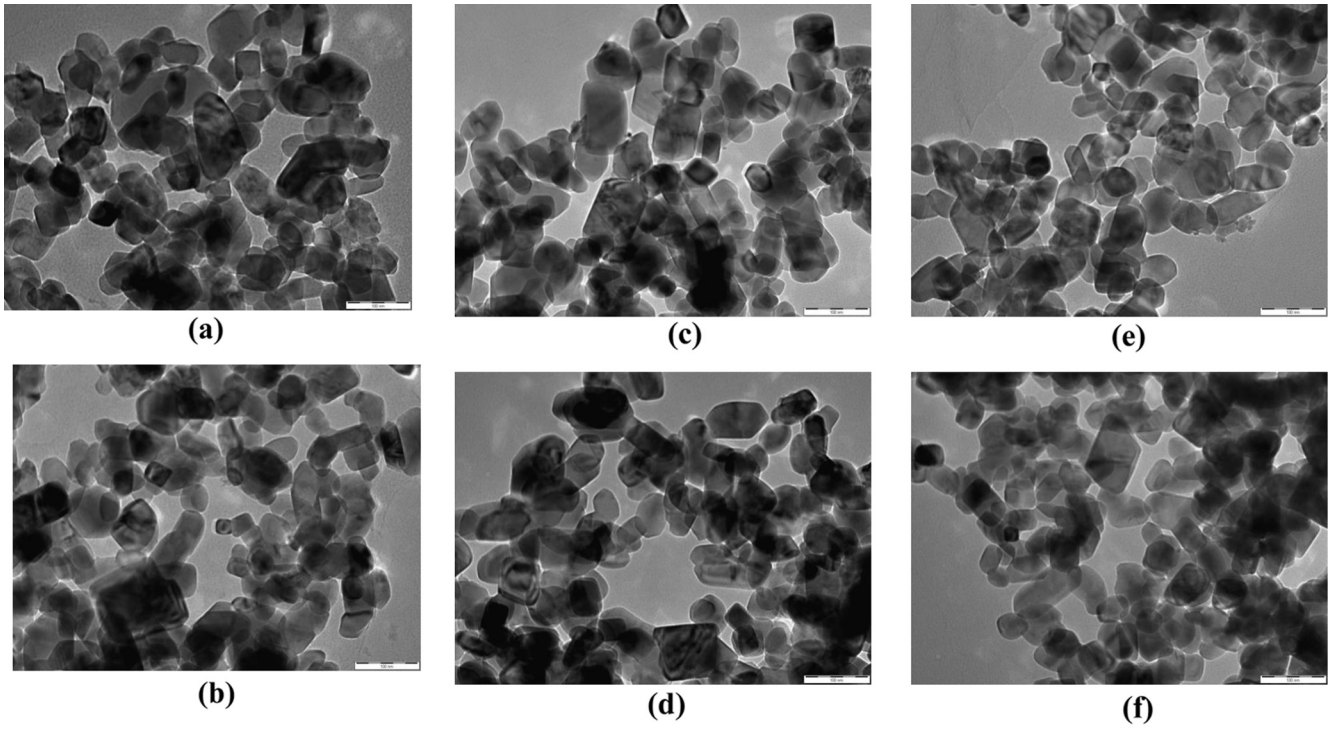

Fig. 2. TEM images of TiO_2 nanofluid with ×140,000 magnification. (a) 1.0% before experiment. (b) 1.0% after experiment. (c) 2.0% before experiment. (d) 2.0% after experiment. (e) 3.0% before experiment. (f) 3.0% after experiment.

4.2. Thermo-physical properties

Sharma et al. [22] developed equations for the estimation of viscosity and thermal conductivity given by Eqs. (5) and (6) respectively for water based nanofluids, using the experimental data of various investigators. The equations are valid for concentration $\phi \leq 4\%$, liquid temperature $T_{nf} \leq 70$ °C of diameter $d_p \leq 170$ nm. The equations have the flexibility to estimate the properties of metal and metal oxide nanofluids dispersed in water. They are given as:

$$\mu_r = \frac{\mu_{nf}}{\mu_w} = \left(1+\frac{\phi}{100}\right)^{11.3}\left(1+\frac{T_{nf}}{70}\right)^{-0.038}\left(1+\frac{d_p}{170}\right)^{-0.061} \tag{5}$$

$$k_r = \frac{k_{nf}}{k_w} = 0.8938\left(1+\frac{\phi}{100}\right)^{1.37}\left(1+\frac{T_{nf}}{70}\right)^{0.2777} \times \left(1+\frac{d_p}{150}\right)^{-0.0336}\left(\frac{\alpha_p}{\alpha_w}\right)^{0.01737} \tag{6}$$

The experimental values of viscosity and thermal conductivity are in satisfactory agreement with values estimated with Eqs. (5) and (6) and used in the analysis. The deviation between experimental data and the values estimated with Eqs. (5) and (6) is less than 1% and 5% respectively for thermal conductivity and viscosity.

4.3. Friction factor

The values recorded by the pressure transducer for flow in a tube and with twisted tape inserts are estimated with Darcy equation given by

$$f = \frac{2D\Delta P}{\rho \bar{V}^2 L} \tag{7}$$

The experimental values of friction factor in the turbulent range for flow of water in the tube are compared with Blasius [23] equation given by

$$f = 0.3164/Re^{0.25} \tag{8}$$

The friction factor for flow over twisted tape inserts is compared with the equation of Smithberg and Landis [24] given by

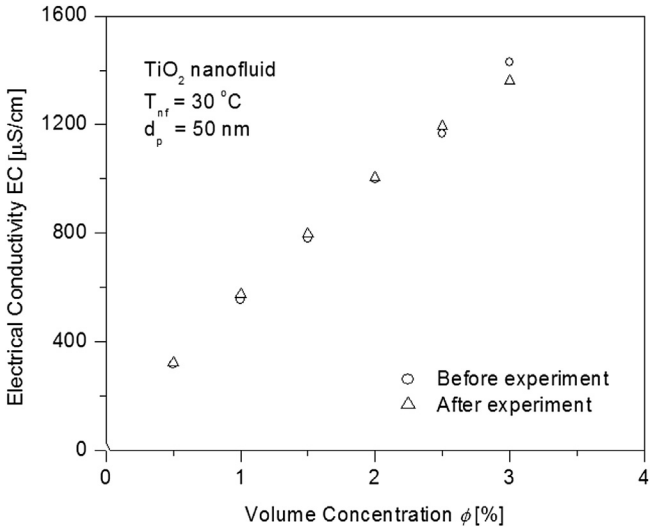

Fig. 3. Electrical conductivity of TiO_2/water nanofluid at 30 °C.

$$f_{SL} = 4\left\{0.046 + 2.1\left[\frac{H}{D} - 0.5\right]^{-1.2}\right\}\left[\frac{Re}{1+2/\pi}\right]^{-n} \tag{9}$$

where $n = 0.2[1 + 1.7(H/D)^{-0.5}]$.

The friction factor of water and TiO_2 nanofluid evaluated with Eq. (7) for flow in a tube and with twisted tape insert are shown through Figs.4–6. The experimental values of friction factor with Reynolds number for water in comparison with Eqs. (8) and (9) are presented as Fig. 4 for flow in a tube and with tape insert respectively. The variation of friction factor with Reynolds number for $H/D = 0$ and 5 at different concentrations are shown as Fig. 5. The values of nanofluid friction factor are higher than those of water and the values with twisted tape inserts are greater than flow in a tube. The friction factor increases with decrease in twist ratio for water and nanofluid.

An equation for the estimation of friction factor for flow of water and TiO_2 nanofluid over tape inserts is developed. The equation is obtained with an average deviation of 5.0%, standard deviation of 5.7% and a maximum deviation of 16.4% given by

$$\frac{f_{nf}}{f_{SL}} = 1.4\left(0.001 + \frac{\phi}{100}\right)^{0.05} \tag{10}$$

valid in the range of $6800 < Re < 30000$, $5.00 \leq Pr \leq 7.24$, $\phi \leq 3\%$ and $5 \leq (H/D) \leq 15$.

The variation of friction factor with Reynolds number for nanofluid at 1.0% concentration is shown in Fig. 6 at different twist ratios. A good agreement of the experimental data with the lines drawn with Eq. (10) is shown confirming the validity of the equation developed.

4.4. Heat transfer coefficients in a tube with water

The energy supplied by the heater and that absorbed by the liquid is validated with the aid of Eq. (11)

$$Q = V \times I \approx \dot{m} C_p (T_e - T_i) \tag{11}$$

The difference between the electrical energy supplied and energy absorbed by the liquid is less than 2.0%. Neglecting the heat loss to the atmosphere, the heat transfer coefficients and the Nusselt number are respectively estimated for water and nanofluids with Eqs. (12) and (13).

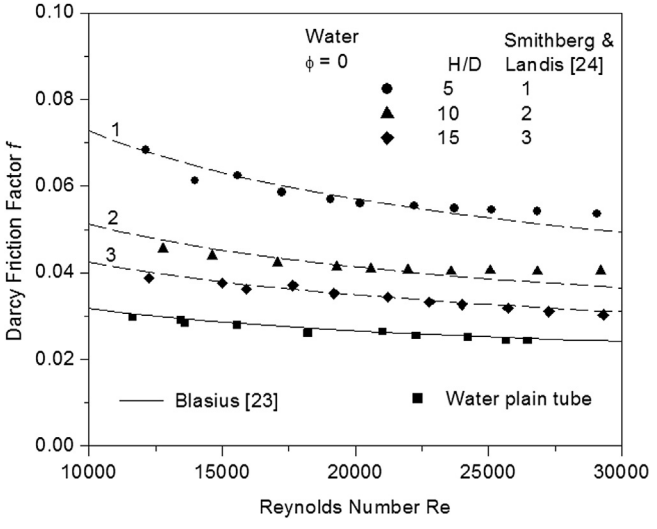

Fig. 4. Comparison of experimental values of friction factor of water with Smithberg and Landis [24] Eq. (9).

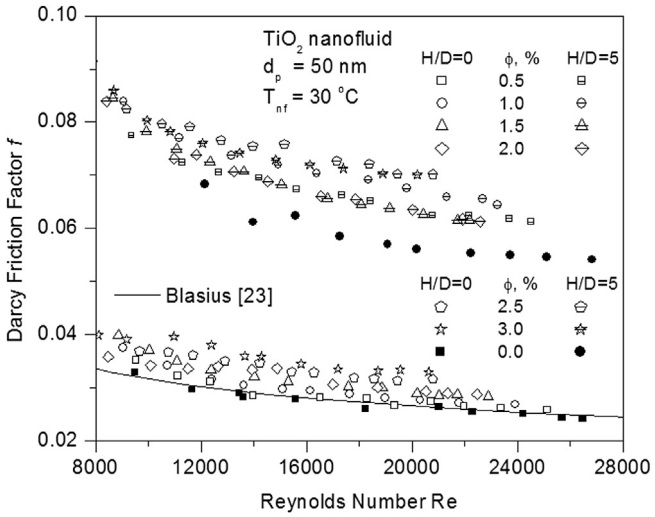

Fig. 5. Experimental friction factor of nanofluid with twisted tapes at H/D of 5.

$$h_{exp} = \frac{Q}{A_s(T_s - T_b)} \tag{12}$$

$$Nu_{exp} = \frac{h_{exp}D}{k} \tag{13}$$

The equation of Dittus and Boelter [25] is widely used for the estimation of Nusselt number of single phase fluids for flow in a tube is given by:

$$Nu = 0.023Re^{0.8}Pr^{0.4} \tag{14}$$

The Eq. (14) is valid for $Re > 10^4$ and $0.6 < Pr < 200$. Further, the equation of Gnielinski [26] for the estimation of Nusselt number for flow in a tube is given as:

$$Nu = \frac{\left(\frac{f}{8}\right)(Re-1000)\mathrm{Pr}}{1+12.7\left(\frac{f}{8}\right)^{0.5}(Pr^{2/3}-1)} \quad \text{where } f = (0.79\ln Re - 1.64)^{-2} \tag{15}$$

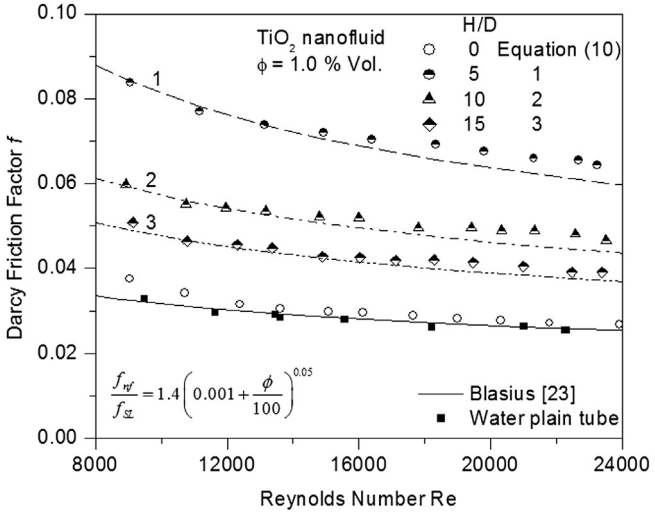

Fig. 6. Comparison of experimental friction factor at 1.0% concentration with the values evaluated from Eq. (10).

which is valid in the range $2300 < Re < 5 \times 10^6$ and $0.5 < Pr < 2000$.

The equation of Sarma et al. [27] applicable for flow over twisted tape inserts, valid in the range of $10{,}000 < Re < 1.3 \times 10^5$ and $3 < Pr < 5$ is expressed as

$$Nu = 0.1012\left(1+\frac{D}{H}\right)^{2.065} Re^{0.67}Pr^{1/3} \tag{16}$$

The equation of Manglik and Bergles [28] valid in the range of $Re \geq 10{,}000$, $Pr = 5.2$(water) and $3 < H/D < 6$ is given by

$$Nu = 0.023Re^{0.8}Pr^{0.4}\left[1+0.769\frac{2D}{H}\right]\phi_2 \tag{17}$$

where, $\phi_2 = [\pi/(\pi - 4\delta/D)]^{0.8}[(\pi + 2 - 2\delta/D)/(\pi - 4\delta/D)]^{0.2}$

Eqs. (12) and (13) are used in the estimation of heat transfer coefficient and Nusselt number of water and nanofluids respectively for flow in a tube and with inserts. Experiments are undertaken with twist ratios of 5, 10 and 15 at different mass flow rates of water. Fig. 7 shows the comparison of the experimental Nusselt number with the equations of Sarma et al. [27] and Manglik and Bergles [28] for water. A satisfactory agreement of the experimental data of water with Eqs. (16) and (17) confirms the validity of the measurements. As the reliability and accuracy of the experimental data with water established, experiments are undertaken with TiO_2 nanofluid to determine the convective heat transfer coefficients.

4.5. Influence of concentration on heat transfer coefficient

Experimental correlations for Nusselt number developed by Pak and Cho [5] and Duangthongsuk and Wongwises [11] are respectively presented with Eqs. (18) and (19), for flow of TiO_2/water nanofluid in a tube under turbulent flow conditions. The equations are:

$$Nu_{nf} = 0.021Re_{nf}^{0.8}Pr_{nf}^{0.5} \tag{18}$$

valid in the range of 0–3.0 vol.%, $10{,}000 < Re < 10^5$ and $6.54 < Pr < 12.33$.

$$Nu_{nf} = 0.074Re_{nf}^{0.707}Pr_{nf}^{0.385}\phi^{0.074} \tag{19}$$

valid in the range of 0–1.0% concentration and $3000 < Re < 18{,}000$. The data from the present experimental setup is in good agreement with the Eqs. (18) and (19) for 1.0% concentration shown in Fig. 8.

The experimental heat transfer coefficients for flow of TiO_2/water nanofluid in a tube at various concentrations estimated with Eq. (12) is shown plotted in Fig. 9. It can be observed that the heat transfer coefficient increases with Reynolds number for volume concentrations up to 1.0%. The enhancement in heat transfer coefficient at 1.0% volume concentration is 23% as shown in Table 2 in the range of Reynolds number tested. At 1.5% concentration, the heat transfer coefficients are lower than those obtained at 1.0%. Further increase in concentration to 2.5% decreased the heat transfer coefficient values to those of water. The values of heat transfer coefficient are lower than water at 3.0% volume concentration.

Similar observation of decrease in Nusselt numbers with increase in concentration of TiO_2 nanofluid is observed by Duangthongsuk and Wongwises [11]. They observed an increase in Nusselt number up to 1.0% concentration with enhancement ranging between 20% and 32%. The Nusselt number decreased with further increase in concentration. They observed the heat transfer coefficient at 25 °C for 2.0% volume concentration to be approximately 14% lower than water under similar operating conditions.

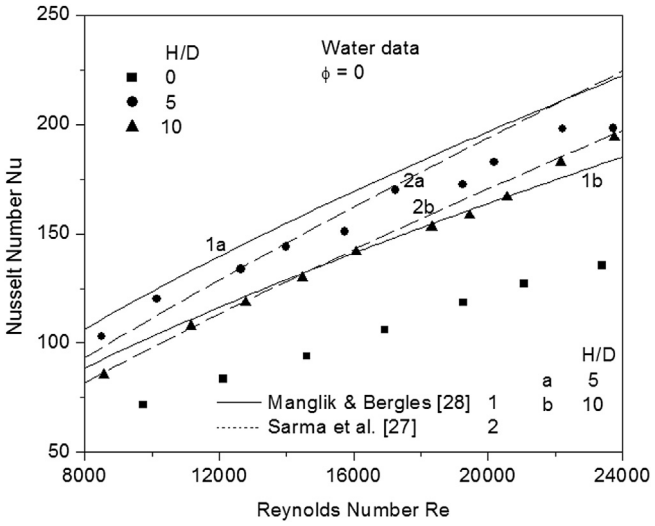

Fig. 7. Comparison of experimental values of twisted tape Nusselt numbers for water with other equations in literature.

4.6. Convective heat transfer coefficient with twisted tapes

Further experiments are undertaken with nanofluids at various twist ratios and flow rates for the determination of heat transfer coefficients and friction factor. The heat transfer coefficient of water and nanofluid is shown in Fig. 9 for twist ratio of 5. Fig. 9 indicates greater values of heat transfer coefficients with twisted tape insert compared to values for flow in a tube. The heat transfer coefficient increases with Reynolds number and decreases with twist ratio. The effect of twist ratio on the Nusselt number is shown in Fig. 10 for 1.0% and 3.0% volume concentrations. It can be observed that Nusselt number decreases with an increase in twist ratio at both concentrations. The values of Nusselt number at 1.0% concentration are greater than the values at 3.0% for the same twist ratio.

A generalized regression equation for the estimation of Nusselt number of water and TiO_2/water nanofluid in a tube with twisted tape insert is developed. The equation is applicable for nanofluid up to 3.0% volume concentration. The equation is obtained with 321 data points with an average deviation of 4.5%, standard deviation of 5.7% and maximum deviation of 13.5% given by

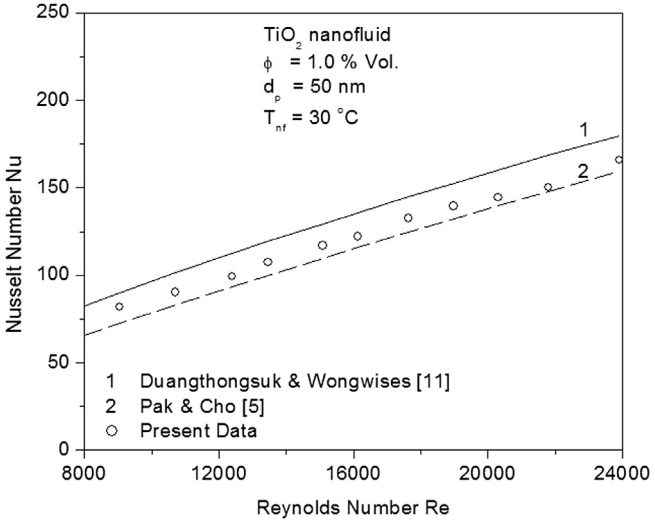

Fig. 8. Comparison of experimental values of Nusselt number with other equations in literature for flow in a tube.

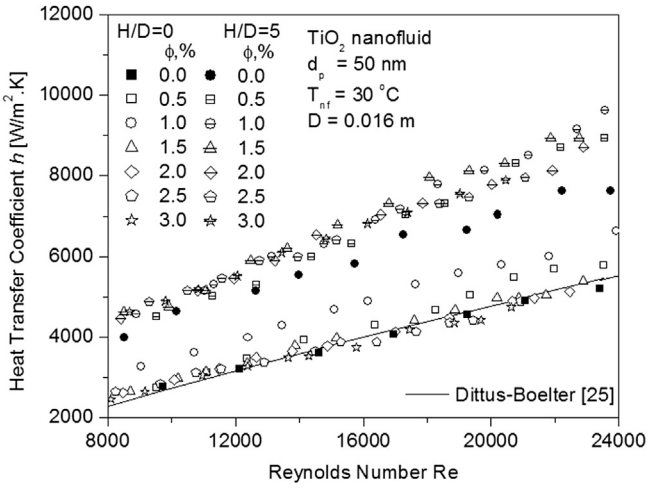

Fig. 9. Variation of TiO_2 nanofluid heat transfer coefficient with Reynolds number for flow in a tube and with twisted tape at various concentration.

$$Nu_{nf} = \frac{h_{nf}D}{k_{nf}} = 0.27Re^{0.693}Pr_{nf}^{-0.3}\left(1+\frac{D}{H}\right)^{1.3} \quad (20)$$

The Nusselt number estimated with Eq. (20) is in good agreement with the experimental data as shown in Fig. 11, thus validating the equation proposed.

The concentration at which the nanofluid is advantageous from the point of view of combined heat transfer and pressure drop is determined with Advantage Ratio, AR. Advantage Ratio of a nanofluid flow in a plain tube AR_{PT}, is the ratio of enhancement in heat transfer coefficient to pressure drop compared to values obtained with base liquid water. In the case of flow with insert, the Advantage Ratio AR_{TT} is the enhancement obtained with a twisted tape insert in comparison to flow of water in the tube. The equations are given as

Table 2
Advantage ratio for flow in a tube and with twisted tape insert at maximum heat transfer coefficient.

Twist ratio H/D	Concentration, ϕ	Heat transfer enhancement	Pressure drop enhancement	Re	AR
0	0.0	–	–	–	–
	0.5	0.10	0.05	25,122	1.74
	1.0	0.23	0.12	23,917	1.88
	1.5	0.04	0.19	22,883	0.20
	2.0	0.03	0.24	22,463	0.12
	2.5	0.02	0.34	21,057	0.05
	3.0	−0.01	0.44	20,626	−0.02
5	0.0	0.51	1.27	29,075	0.40
	0.5	0.69	1.47	24,595	0.47
	1.0	0.81	1.67	23,558	0.48
	1.5	0.74	1.62	22,469	0.46
	2.0	0.68	1.64	22,127	0.41
	2.5	0.64	1.98	20,824	0.32
	3.0	0.66	2.01	20,328	0.33
10	0.0	0.39	0.67	29,209	0.59
	0.5	0.62	0.90	24,682	0.69
	1.0	0.66	0.93	23,698	0.71
	1.5	0.45	1.02	22,694	0.44
	2.0	0.60	1.06	22,321	0.56
	2.5	0.58	1.25	20,933	0.46
	3.0	0.53	1.39	20,456	0.38
15	0.0	0.33	0.43	29,307	0.76
	0.5	0.50	0.59	24,829	0.85
	1.0	0.55	0.61	23,821	0.90
	1.5	0.39	0.72	22,856	0.54
	2.0	0.51	0.74	22,887	0.68
	2.5	0.31	0.93	21,057	0.33
	3.0	0.46	1.21	20,553	0.38

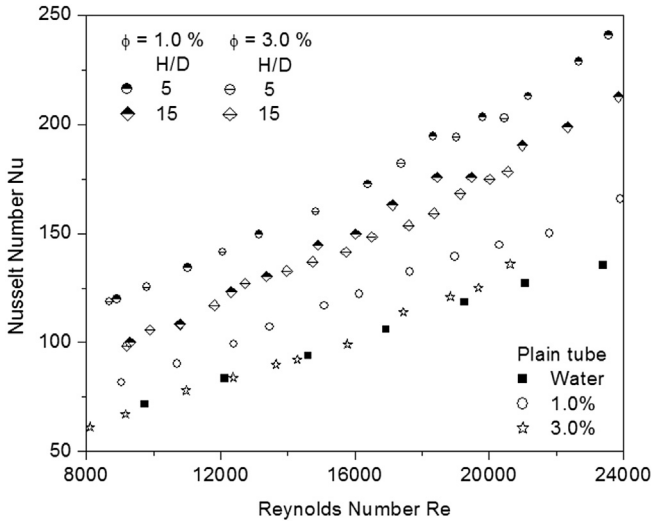

Fig. 10. Effect of H/D ratio on experimental Nusselt numbers at 1.0% and 3.0% concentration.

$$\text{Advantage Ratio, AR} = \frac{\text{htc enhancement ratio}}{\text{pressure drop enhancement ratio}} \tag{21}$$

$$\text{Plain Tube Advantage Ratio, } AR_{PT} = \left(\frac{h_{PT(nf)} - h_{PT(w)}}{h_{PT(w)}}\right) \Big/ \left(\frac{\Delta P_{PT(nf)} - \Delta P_{PT(w)}}{\Delta P_{PT(w)}}\right) \tag{22}$$

$$\text{Twisted Tape Advantage Ratio, } AR_{TT} = \left(\frac{h_{TT(nf)} - h_{PT(w)}}{h_{PT(w)}}\right) \Big/ \left(\frac{\Delta P_{TT(nf)} - \Delta P_{PT(w)}}{\Delta P_{PT(w)}}\right) \tag{23}$$

The values of advantage ratio AR_{PT} and AR_{TT} estimated respectively with Eqs. (22) and (23) at maximum values of heat transfer coefficient are given in Table 2 at different concentrations and twist ratios.

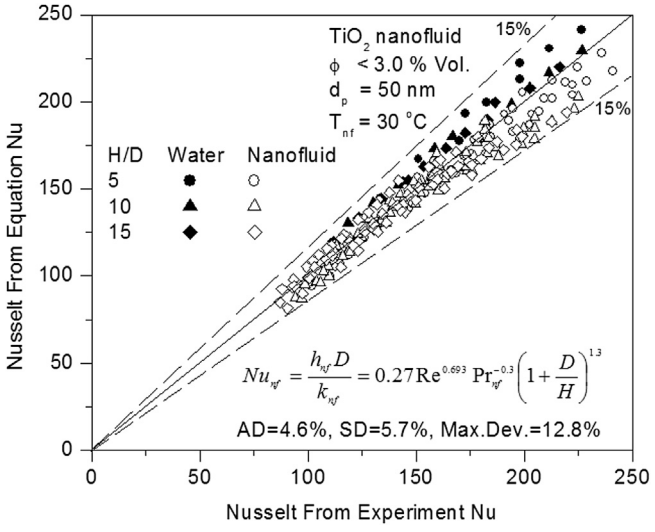

Fig. 11. Validation of experimental data with Eq. (20).

5. Conclusions

Experiments are undertaken with TiO_2 for flow of nanofluid in a tube and with tape inserts for the determination of heat transfer coefficients and friction factor in the turbulent range of Reynolds numbers. The nanofluid heat transfer coefficients in the Reynolds number range of 8000 and 30,000 increased with volume concentration up to 1.0% and decreased at higher concentrations for flow in a tube. The maximum enhancement in heat transfer coefficient at 1.0% volume concentration is 23.2% at the Reynolds number of 23,917 for flow in a tube. The increase in friction factor is 5% under similar operating conditions. For flow over tape insert of twist ratio 5, the maximum enhancement in heat transfer coefficient is 81.1% compared to water and 48.1% with nanofluid at 1.0% concentration. The nanofluid friction factor with twist ratio of 5 is greater than twice the value obtained for flow of water in a tube at $Re = 23{,}558$. Sundar and Sharma [14] observed the friction factor with Al_2O_3 nanofluid of 0.5% volume concentration and twist ratio five to be 1.096 times greater compared to flow of water in a tube. However, Wongcharee and Eiamsa-ard [15] reported the heat transfer enhancement of 44.9% with CuO nanofluid at 0.7% concentration and $Re = 23{,}200$ for flow in a corrugated tube with twisted tape insert of $H/D = 5.3$; whereas the friction factor is 3.8 times greater compared to flow of nanofluid in the tube.

A comparison of heat transfer enhancements for flow of nanofluid in a tube with twisted tape insert is made considering pressure drop with Advantage Ratio AR. The maximum AR_{PT} of 1.88 is obtained with 1.0% concentration at the operating temperature of 30 °C for flow of TiO_2 nanofluid in a tube. However, with tape insert of twist ratio 15 under similar conditions of concentration and operating temperature, the maximum AR value obtained is 0.90. For flow with twisted tape inserts, the AR increases with twist ratio for both water and nanofluid. Hence, from the values of Advantage Ratio estimated, it is preferable to have the flow of TiO_2 nanofluid at 1.0% concentration in a tube. However, at the same concentration with tape insert of twist ratio 5, the maximum enhancement in heat transfer coefficient is 81%.

Acknowledgments

The financial support by Universiti Malaysia Pahang under GRS100354 and RDU130391 are gratefully acknowledged. The corresponding author thank Jawaharlal Nehru Technological University Hyderabad for the academic support rendered in this regard.

Nomenclature

A	area, m^2
AR	advantage ratio
C	specific heat, J/kg K
d_p	diameter of nanoparticle, nm
D	tube inner diameter, m
f	Darcy friction factor, $((D/L)(\Delta P)/(\rho \bar{V}^2/2))$
f_{SL}	Smithberg and Landis friction factor
H	helical pitch of the twisted tape for 180° rotation, m
h	heat transfer coefficient, W/m^2 K
ID	inner diameter, m
k	thermal conductivity, W/m K
k_r	thermal conductivity ratio of nanofluid to water, (k_{nf}/k_w)
L	tube length, m
LPM	liter per minute
Nu	Nusselt number, (hD/k)
OD	outer diameter, m
Pr	Prandtl number, $(\mu C/k)$
Q	heat input, W
Re	Reynolds number, $(\rho \bar{V} D/\mu)$
T	temperature, °C

U	uncertainty
TEM	transmission electron microscopy
V_1	initial volume, L
V_2	final volume, L
$\overline{V}$	average velocity, m/s

Greek symbols

α	thermal diffusivity, m^2/s
δ	thickness of strip, m
ΔP	pressure drop, Pa
ΔV	volume of distilled water for dilution, L
ϕ	volume concentration, %
ϕ_1	initial volume concentration, %
ϕ_2	final volume concentration, %
φ	volume fraction, $\varphi = (\phi/100)$
μ	absolute viscosity, kg/m s
μ_r	ratio of nanofluid to water viscosity, (μ_{nf}/μ_w)
ρ	density, kg/m^3
ω	weight concentration, %

Subscripts

b	average
e	exit
exp	experiment
i	inlet
nf	nanofluid
p	particle
PT	plain tube
r	ratio
s	surface
TT	twisted tape
w	water

Appendix 1. Uncertainties of instruments.

No.	Name of instrument	Range of instrument	Variable measured	Least division in measuring instrument	Values measured in experiment		% uncertainty	
					Min	Max	Max	Min
1	Thermocouple	0–300 °C	Bulk temperature, T_b	$U_T = 0.1\ ^\circ C$ $U_{Tb} = \sqrt{0.1^2 + 0.1^2}$ $= 0.14142\ ^\circ C$	28.75	31.25	0.49190	0.45255
2	Thermocouple	0–300 °C	Average surface temperature, T_w	$U_T = 0.1\ ^\circ C$ $U_{T_w} = \sqrt{5 \times (0.1^2)}$ $= 0.22361$	29.83	34.53	0.74960	0.64757
3	Flowmeter	2–30 LPM	Volume flow rate, $\dot{V}$ Velocity, $\overline{V}$	0.1	5	17.8	2.0	0.56180
4	Voltage	0–240 V	Voltage, V	0.01	110.1	110.1	0.00908	0.00908
5	Current	0–15 A	Current, I	0.01	5.45	5.45	0.18348	0.18348
6	Pressure transducer	0–16.2 mV	Voltage, mV	0.01	0.57	11.46	1.75439	0.08726
		0–6894.8 Pa (0–1 Psi)	Pressure Drop, ΔP	–	332	4904.37	1.75439	0.08726

Appendix 2. Uncertainty of physical quantities.

No.	Heat transfer and friction parameter	Maximum uncertainty (%)	Minimum uncertainty (%)
1	Reynolds number, Re $Re = \frac{\rho \overline{V} D}{\mu}$	$\frac{U_{Re}}{Re} = \sqrt{\left(\frac{U_\rho}{\rho}\right)^2 + \left(\frac{U_{\overline{V}}}{\overline{V}}\right)^2 + \left(\frac{U_\mu}{\mu}\right)^2}$ $= \sqrt{(0.1)^2 + (2.0)^2 + (0.1)^2}$ $= 2.0050\%$	$\frac{U_{Re}}{Re} = \sqrt{\left(\frac{U_\rho}{\rho}\right)^2 + \left(\frac{U_{\overline{V}}}{\overline{V}}\right)^2 + \left(\frac{U_\mu}{\mu}\right)^2}$ $= \sqrt{(0.1)^2 + (0.56180)^2 + (0.1)^2}$ $= 0.57932\%$
2	Heat flux, q $q = Q/A = VI/\pi DL$	$\frac{U_q}{q} = \sqrt{\left(\frac{U_V}{V}\right)^2 + \left(\frac{U_I}{I}\right)^2}$ $= \sqrt{(0.00908)^2 + (0.18348)^2}$ $= 0.18371\%$	$\frac{U_q}{q} = \sqrt{\left(\frac{U_V}{V}\right)^2 + \left(\frac{U_I}{I}\right)^2}$ $= \sqrt{(0.00908)^2 + (0.18348)^2}$ $= 0.18371\%$
3	Heat transfer coefficient, h $h = q/(T_w - T_b)$	$\frac{U_h}{h} = \sqrt{\left(\frac{U_q}{q}\right)^2 + \left(\frac{U_{(T_w - T_b)}}{(T_w - T_b)}\right)^2}$ $\frac{U_{(T_w - T_b)}}{(T_w - T_b)} = \sqrt{(0.74960)^2 + (0.49190)^2}$ $= 0.89659\%$ $\frac{U_h}{h} = \sqrt{(0.18371)^2 + (0.89659)^2}$ $= 0.91522\%$	$\frac{U_h}{h} = \sqrt{\left(\frac{U_q}{q}\right)^2 + \left(\frac{U_{(T_w - T_b)}}{(T_w - T_b)}\right)^2}$ $\frac{U_{(T_w - T_b)}}{(T_w - T_b)} = \sqrt{(0.64757)^2 + (0.45255)^2}$ $= 0.79003\%$ $\frac{U_h}{h} = \sqrt{(0.18371)^2 + (0.79003)^2}$ $= 0.81111\%$
4	Nusselt number, Nu $Nu = hD/k$	$\frac{U_{Nu}}{Nu} = \sqrt{\left(\frac{U_h}{h}\right)^2 + \left(\frac{U_k}{k}\right)^2}$ $= \sqrt{(0.91522)^2 + (0.1)^2}$ $= 0.92066\%$	$\frac{U_{Nu}}{Nu} = \sqrt{\left(\frac{U_h}{h}\right)^2 + \left(\frac{U_k}{k}\right)^2}$ $= \sqrt{(0.81111)^2 + (0.1)^2}$ $= 0.81725\%$
5	Friction factor, f $f = \frac{\Delta P}{\left(\frac{L}{D}\right)\left(\frac{\rho \overline{V}^2}{2}\right)}$	$\frac{U_f}{f} = \sqrt{\left(\frac{U_{\Delta P}}{\Delta P}\right)^2 + \left(\frac{U_\rho}{\rho}\right)^2 + \left(\frac{U_{\overline{V}}}{\overline{V}}\right)^2}$ $= \sqrt{(1.75439)^2 + (0.1)^2 + (2.0)^2}$ $= 4.36897\%$	$\frac{U_f}{f} = \sqrt{\left(\frac{U_{\Delta P}}{\Delta P}\right)^2 + \left(\frac{U_\rho}{\rho}\right)^2 + \left(\frac{U_{\overline{V}}}{\overline{V}}\right)^2}$ $= \sqrt{(0.08726)^2 + (0.1)^2 + (0.56180)^2}$ $= 1.13141\%$
6	Thermo physical properties	0.1	0.1

References

[1] A.S. Ahuja, Augmentation of heat transport in laminar flow of polystyrene suspensions. I. Experiments and results, J. Appl. Phys. 46 (8) (1975) 3408–3416.

[2] A.E. Bergles, Techniques to augment heat transfer, in: W.M. Rohsenow, J.P. Hartnett, E.N. Ganic (Eds.), Handbook of Heat Transfer Applications, McGraw-Hill, New York, 1985, pp. 31–380.

[3] U. Choi, T. Tran, Experimental studies of the effects of non-Newtonian surfactant solutions on the performance of a shell-and-tube heat exchanger, Recent Dev. Newt. Flows Ind. Appl. 124 (1991) 47–52.

[4] H. Masuda, A. Ebata, K. Teramae, N. Hishinuma, Alteration of Thermal conductivity and viscosity of liquid by dispersing ultra fine particles, Netsu Bussei 4 (4) (1993) 227–233.

[5] B.C. Pak, Y.I. Cho, Hydrodynamic and heat transfer study of dispersed fluids with submicron metallic oxide particles, Exp. Heat Transfer 11 (2) (1998) 151–170.

[6] A. Turgut, I. Tavman, M. Chirtoc, H.P. Schuchmann, C. Sauter, S. Tavman, Thermal conductivity and viscosity measurements of water-based TiO_2 nanofluids, Int. J. Thermophys. 30 (2009) 1213–1226.

[7] Y. He, Y. Men, Y. Zhao, H. Lu, Y. Ding, Numerical investigation into the convective heat transfer of TiO_2 nanofluids flowing through a straight tube under the laminar flow conditions, Appl. Therm. Eng. 29 (10) (2009) 1965–1972.

[8] Y. He, Y. Jin, H. Chen, Y. Ding, D. Cang, H. Lu, Heat transfer and flow behaviour of aqueous suspensions of TiO_2 nanoparticles (nanofluids) flowing upward through a vertical pipe, Int. J. Heat Mass Transfer 50 (11–12) (2007) 2272–2281.

[9] M.H. Kayhani, H. Soltanzadeh, M.M. Heyhat, M. Nazari, F. Kowsary, Experimental study of convective heat transfer and pressure drop of TiO_2/water nanofluid, Int. Commun. Heat Mass Transfer 39 (3) (2012) 456–462.

[10] A.A.A. Arani, J. Amani, Experimental study on the effect of TiO_2–water nanofluid on heat transfer and pressure drop, Exp. Therm. Fluid Sci. 42 (0) (2012) 107–115.

[11] W. Duangthongsuk, S. Wongwises, An experimental study on the heat transfer performance and pressure drop of TiO_2–water nanofluids flowing under a turbulent flow regime, Int. J. Heat Mass Transfer 53 (1–3) (2010) 334–344.

[12] W.H. Azmi, K.V. Sharma, P.K. Sarma, R. Mamat, S. Anuar, V. Dharma Rao, Experimental determination of turbulent forced convection heat transfer and friction factor with SiO_2 nanofluid, Exp. Therm. Fluid Sci. 51 (0) (2013) 103–111.

[13] K.V. Sharma, L.S. Sundar, P.K. Sarma, Estimation of heat transfer coefficient and friction factor in the transition flow with low volume concentration of Al_2O_3 nanofluid flowing in a circular tube and with twisted tape insert, Int. Commun. Heat Mass Transfer 36 (5) (2009) 503–507.

[14] L.S. Sundar, K.V. Sharma, Turbulent heat transfer and friction factor of Al_2O_3 nanofluid in circular tube with twisted tape inserts, Int. J. Heat Mass Transfer 53 (7–8) (2010) 1409–1416.

[15] K. Wongcharee, S. Eiamsa-ard, Heat transfer enhancement by using CuO/water nanofluid in corrugated tube equipped with twisted tape, Int. Commun. Heat Mass Transfer 39 (2) (2012) 251–257.

[16] H.A. Mintsa, G. Roy, C.T. Nguyen, D. Doucet, New temperature dependent thermal conductivity data for water-based nanofluids, Int. J. Therm. Sci. 48 (2) (2009) 363–371.

[17] P.K. Namburu, D.P. Kulkarni, D. Misra, D.K. Das, Viscosity of copper oxide nanoparticles dispersed in ethylene glycol and water mixture, Exp. Therm. Fluid Sci. 32 (2) (2007) 397–402.

[18] Y. Ding, H. Alias, D. Wen, R.A. Williams, Heat transfer of aqueous suspensions of carbon nanotubes (CNT nanofluids), Int. J. Heat Mass Transfer 49 (1–2) (2006) 240–250.

[19] Y.A. Cengel, M.A. Boles, M. Kanoğlu, Thermodynamics: an Engineering Approach, vol. 3, McGraw-Hill, New York, 2011.

[20] S.M.S. Murshed, K.C. Leong, C. Yang, Enhanced thermal conductivity of TiO_2–water based nanofluids, Int. J. Therm. Sci. 44 (4) (2005) 367–373.

[21] K.G.K. Sarojini, S.V. Manoj, P.K. Singh, T. Pradeep, S.K. Das, Electrical conductivity of ceramic and metallic nanofluids, Colloids Surf. Physicochem. Eng. Asp. 417 (0) (2013) 39–46.

[22] K.V. Sharma, P.K. Sarma, W.H. Azmi, R. Mamat, K. Kadirgama, Correlations to predict friction and forced convection heat transfer coefficients of water based nanofluids for turbulent flow in a tube, Int. J. Microscale Nanoscale Therm. Fluid Transp. Phenom. 3 (4) (2012) 1–25 (Special issue in Heat and Mass Transfer in Nanofluids).

[23] H. Blasius, Das Aehnlichkeitsgesetz bei Reibungsvorgängen in Flüssigkeiten, Mittl. Forschungsarb. Geb. Ingenieurwes. 131 (1913).

[24] E. Smithberg, F. Landis, Friction and forced convection heat transfer characteristics in tubes with twisted-tape swirl generators, Trans. ASME J. Heat Transfer 86 (1964) 39–49.

[25] F.W. Dittus, L.M.K. Boelter, Heat Transfer in Automobile Radiators of the Tubular Type, vol. 2, University of California Publications on Engineering, 1930, pp. 443–461.

[26] V. Gnielinski, New equations for heat and mass transfer in turbulent pipe and channel flow, Int. Chem. Eng. 16 (1976) 359–368.

[27] P.K. Sarma, T. Subramanyam, P.S. Kishore, V.D. Rao, S. Kakac, A new method to predict convective heat transfer in a tube with twisted tape inserts for turbulent flow, Int. J. Therm. Sci. 41 (10) (2002) 955–960.

[28] R.M. Manglik, A.E. Bergles, Heat Transfer, Pressure drop correlations for twisted-tape inserts in isothermal tubes: part II – transition and turbulent flows, J. Heat Transfer 115 (4) (1993) 890–896.